Inverse Pre-Deformation of Tetrahedral Mesh for Large Deformation Finite Element Analysis

Arbtip Dheeravongkit[1] and Kenji Shimada[2]

[1]Carnegie Mellon University, aom@cmu.edu
[2]Carnegie Mellon University, shimada@cmu.edu

ABSTRACT

In the finite element analysis that involves with large deformation, distorted elements are usually produced in the later stages of the analysis. These distorted elements lead to inaccurate solutions, slow convergence and premature termination of the analysis. This paper proposes an inverse pre-deformation method to generate the input tetrahedral mesh for Lagrangian analysis. By this method, tetrahedral elements in the input mesh are pre-deformed into shapes approximately opposite of those produced in the analysis. As a result, the number of inverted and ill-shaped elements can be reduced at the later stage of the analysis. A pre-analysis is required to collect geometric information and equivalent plastic strain information. The proposed method then generates a new optimal mesh on the deformed boundary, considering equivalent plastic strain information to control mesh sizes, and finally, maps the new elements to the undeformed boundary using barycentric interpolation to create the pre-deformed tetrahedral mesh.

Keywords: Large Deformation Analysis, Mesh generation, Inverse Pre-deformation, Bubble Mesh.

1. INTRODUCTION

The process of finite element analysis that deals with large deformation usually produces distorted elements at the later stages of the analysis. These distorted elements lead to several problems: inaccurate results, slow convergence and premature analysis termination. Metal-forming processes are the most common applications involved with large deformation analysis; they include forging, extrusion, rolling, deep drawing, etc. An example of such large deformation analysis is illustrated in Fig. 1. This is a three-dimensional forging example, containing a sinusoidal die that deforms a deformable blank into geometry with high-curvature corners. As the finite element analysis is performed on this problem using pure Lagrangian method, several elements are severely distorted especially around high-curvature corners. Consequently, the resulting mesh contains many highly-distorted elements at the later stages, leading to several problems listed earlier.
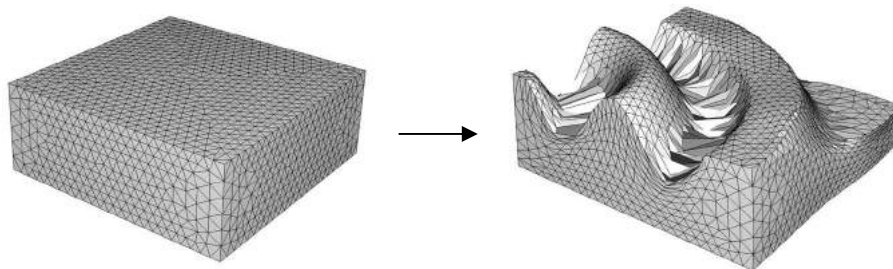
Fig. 1. An example of large deformation finite element analysis (Forging with a sinusoidal die).

As an alternative solution, this paper proposes an "inverse pre-deformation" method to "pre-deform" the input tetrahedral mesh for Lagrangian analysis to reduce the number of inverted and ill-shaped elements at the later stage of the analysis. The term "inverse pre-deformation" is used to illustrate the idea of this method, in which we first predict the way each mesh element will be deformed during analysis, and then create the new input mesh, which contains elements that have approximately opposite shapes of those predicted. In conclusion, this method pre-deforms input

mesh elements into shapes approximately opposite of which they will ultimately be deformed. With this approach, the number of inverted and ill-shaped elements in the later analysis stage can be reduced, because overall element shape quality tends to improve along the analysis process.

The two-dimensional version of this inverse pre-deformation method was proposed earlier to generate the input quadrilateral mesh for large deformation analysis. It has been proved that the inverse pre-deformation method can successfully extend the life of the analysis, as well as reduce the number of ill-shaped elements at the later stage [19]. The work presented in this paper shows that a similar concept can be used to generate the tetrahedral mesh for three-dimensional problems. However, there are some major differences between the two-dimensional and three-dimensional pre-deformation methods, which will be explained in detail in section 2. Nevertheless, there are two conventional techniques for addressing this problem, the adaptive remeshing and the Arbitrary Lagrangian-Eulerian (ALE). However, both techniques have drawbacks.

Adaptive remeshing is a technique, which replaces an over-distorted mesh with a better-conditioned mesh when the error approximation of analysis exceeds the tolerance, or the maximum error value allowed [2]. The newly- created mesh may not necessarily have the same topology as the original mesh, and the number of nodes and elements of the new mesh may differ from the original mesh. Therefore, state variables and history-dependent variables must also be transferred from the original to the new mesh. State variables include nodal displacements and variables of the contact algorithm. History-dependent variables are the stress tensor, strain tensor, plastic strain tensor, etc. The adaptive remeshing technique usually completely re-meshes the part at every certain number of steps in the analysis [1-3]. The disadvantage of this method is its high computational cost, especially during the procedure for determining the error estimator and mapping variables from an old to a new mesh [3]. More importantly, computational costs increase considerably for analysis of complicated geometries.

The Arbitrary Lagrangian-Eulerian (ALE) method is another technique for addressing the problem of large deformation in finite element analysis. This method combines the features of pure Lagrangian analysis and Eulerian analysis--two common types of finite element analysis. In pure Lagrangian analysis, a mesh follows the material deformation during analysis; the mesh is connected to the material throughout the finite element calculation [5]. Since the mesh and the material are connected, severe distortion of the mesh can cause difficulty in the finite element calculation. It is here that adaptive remeshing must be applied to improve the shape quality of the mesh in order to continue the analysis. ALE was developed to reduce the repetition of complete remeshing [4-8]. Essentially, ALE is a Lagrangian analysis that takes advantage of the advection techniques of Eulerian analysis. In the ALE method, the mesh is neither connected to the material nor fixed to a spatial coordinate system. Rather, it is prescribed in an arbitrary manner [4]. During the analysis, the mesh elements deform according to the Lagrangian method. However, instead of repositioning the nodes at their original position and performing advection, as in the Eulerian method, the nodes are placed at other positions to obtain optimal mesh quality. The mesh nodes have velocity associate with them in order to obtain the updated mesh. Mesh velocity plays an important role in the ALE method, as it reduces the analysis error, and prevents mesh distortion [4]. Another important characteristic of this method is that it changes the location of the nodes in the existing mesh, instead of creating a completely new mesh, like the adaptive remeshing method, and it maintains the same (or similar) mesh topology throughout the analysis [5]. However, because of its complexity, the computation cost is much more expensive than using pure Lagrangian analysis. There are also other limitations in ALE analysis. In many cases the mesh suffers considerable distortion, and the same mesh topology cannot be maintained for the entire analysis. In such cases, complete adaptive remeshing is still required. Another drawback of ALE is that the state-variables remapping step is much more complicated than in the Lagrangian method.

It should be noted that the proposed inverse pre-deformation method is not meant to be a replacement of the previous two existing methods. However, because the inverse pre-deformation method reduces the number of ill-shaped elements, it can hold the analysis to a further step before mesh quality becomes unacceptable where the adaptive remeshing is required. Therefore, the inverse pre-deformed mesh can help to reduce the number of remeshing in the analysis and save computational time due to the remeshing process.

2. INVERSE PRE-DEFORMATION OF TETRAHEDRAL MESH
A new inverse pre-deformation method is proposed here, to generate an input tetrahedral mesh for three-dimensional Lagrangian analysis that expects large deformation. This method produces pre-deformed mesh whose element shapes are approximately inverse from shapes into which they will be deformed during the analysis. Accordingly, the new

analysis, run on the pre-deformed mesh, can reduce the chance of inverted elements at the later stage and decrease the possibility of premature analysis termination.

The method can be summarized in the following four steps:

Step 1   Pre-Analysis: Pre-analysis is run on a simple uniform mesh to predict deformation behavior by collecting node locations and equivalent plastic strain, which gives the deformation intensity information regarding the deformed part.

Step 2   Bubble Mesh: Optimal node locations inside the deformed boundary are found using Bubble Mesh [13-17]. The strain information obtained from Step 1 is used to control the element sizes. Then, an optimal mesh is generated on the deformed boundary.

Step 3   Barycentric interpolation: Barycentric interpolation is used to map node locations generated in the previous step, from the deformed to the undeformed boundary.

Step 4   Full Analysis: Actual analysis is run on the new pre-deformed mesh.

The concept of this proposed method is similar to that of the two-dimensional inverse pre-deformation method presented earlier [19]. The major difference between the previous and current pre-deformation methods is the node mapping process in step 3. The previous method uses inverse bilinear mapping to generate quadrilateral mesh, while the current method uses barycentric interpolation to generate tetrahedral mesh. Moreover, because the deformation behavior of the three-dimensional problem is usually more complicated than the two-dimensional problems, there are more chances that one iteration of pre-deformation might not be enough for adequate results. In this paper, we show that the inverse pre-deformation method can be repeated iteratively to progressively improve the analysis results and extend the life of the analysis to the desired stage. Fig. 2 illustrates the overview of the proposed inverse pre-deformation algorithm.
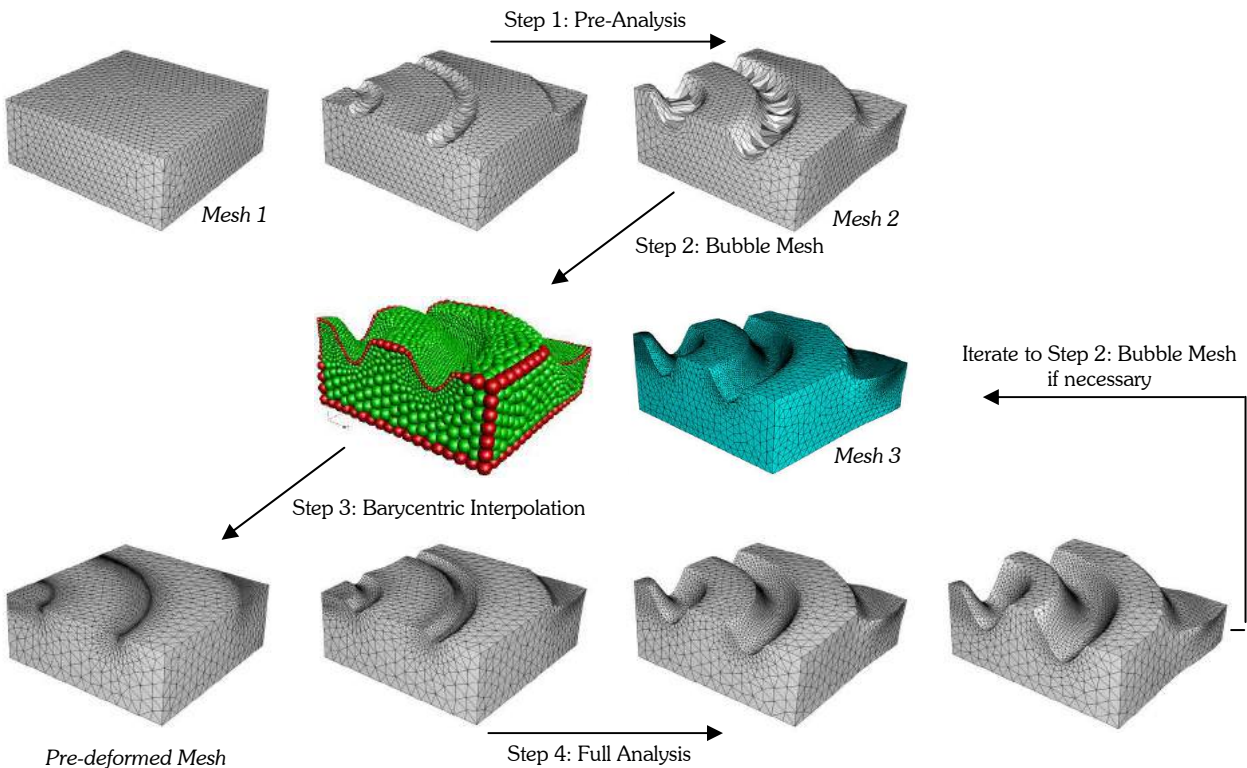
Fig. 2. Overview of Inverse Pre-deformation method.

Following is the concept behind this method: In step 1, pre-analysis is run on a simple uniform mesh to observe how the mesh elements are deformed. In this first step, we keep two mesh data; one is the initial undeformed mesh (Mesh 1), and the other is the deformed mesh (Mesh 2). Then, in step 2, Mesh 2 is replaced with a new optimal mesh (Mesh 3), which is generated using the Bubble Mesh [13-17]. This mesh is the ideal mesh we hope to achieve at that stage of the analysis. At this point, it is known that if we start the analysis from Mesh 1, we get Mesh 2 as the final resulting mesh. However, Mesh 3 is the desired resulting mesh. Therefore, in step 3, we compare Mesh 3 with Mesh 2 by using the barycentric interpolation function to locate each node of Mesh 3 inside Mesh 2. These nodes are then mapped onto Mesh 1 to generate the new initial mesh, which analysis should start from. This new initial mesh is the pre-deformed mesh, on which full analysis is carried out in step 4. Next, we will discuss each step of the algorithm in detail.

2.1 Pre-Analysis
The pre-analysis is carried out on a simple uniform input mesh. It can be run using any finite element package, however, for this paper, ABAQUS has been used for all the example analyses. In addition, the quadratic tetrahedral elements are used because they can tolerate more severe distortion than the linear elements.

The primary goal of the pre-analysis is to predict deformation behavior and collect necessary information, e.g. deformed boundary information and plastic equivalent strain, which will be used in the later pre-deformation steps. Thus, pre-analysis can be carried out until only during 50%-80% of the actual analysis process, or until when the severe distortion starts occurring. Furthermore, two mesh data are maintained in this step; the initial undeformed mesh (Mesh 1), and the deformed mesh (Mesh 2). However, to facilitate the node mapping process in the later step, each quadratic tetrahedral element in Mesh 1 and Mesh 2 is subdivided into eight linear tetrahedral elements.

2.2 Bubble Mesh
In this step, the boundary of the deformed blank obtained from pre-analysis in the first step is used; bubbles are packed inside the boundary and a new optimal tetrahedral mesh (Mesh 3) is generated. Details of Bubble Mesh algorithm can be found in [13-17].

When generating the tetrahedral mesh, the element sizes should be properly determined. Ideally, smaller elements are desirable around the high-curvature corner regions, where they tend to experience more distortion. For this reason, a tetrahedron mesher, which can control the element sizes precisely, is needed. Bubble Mesh can achieve this by utilizing the equivalent plastic strain information collected from pre-analysis to control the mesh sizes over the whole domain through the grid-based tensor function. A background grid is first defined over the domain, where the grid size must be determined properly for each problem. Mesh sizes are then stored at the grid nodes corresponding to the values of the equivalent plastic strain. Smaller element sizes are specified where the equivalent plastic strain values are higher such as around the high-curvature corners. For the internal point of a grid cell, Bubble Mesh calculates the mesh size by linear interpolation of the values at four grid nodes. Bubble mesh packs the sphere bubbles closely inside the boundary of the deformed blank using sizes specified in the tensor function to control the size of the bubbles. The mesh nodes are placed at the centers of the bubbles and are then connected by Delaunay triangulation and tetrahedrization to generate the tetrahedral mesh.

The outcome of this step is a deformed blank, which is optimally meshed into graded tetrahedral elements. Fig. 3 (a) and (b) illustrate the bubble packing processes with size control.

(a) Bubble Packing   (b) Tetrahedral Mesh (Mesh 3)
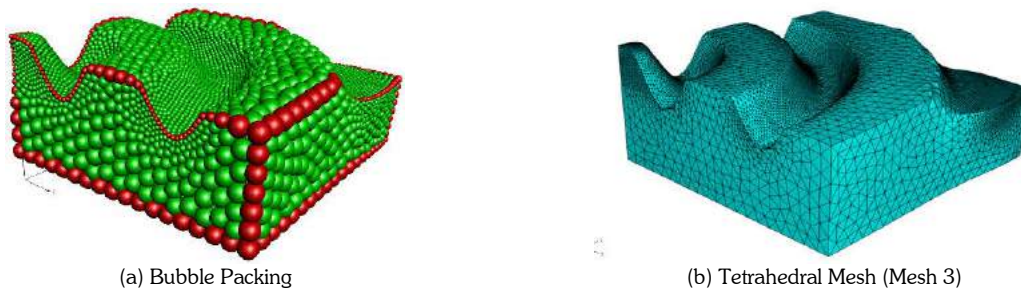
Fig. 3. Sphere Bubble Mesh packing with size control.

2.3 Barycentric Interpolation

In this step, new nodes created by Bubble Mesh are mapped from the deformed blank onto the undeformed blank to generate pre-deformed mesh using barycentric interpolation. We first compare the original deformed mesh (Mesh 2) with the optimal mesh generated by Bubble Mesh (Mesh 3) and locate, using the interpolation function, the position of each Mesh 3's node on Mesh 2. Practically, for each Mesh 3's node, we search on Mesh 2 for the element in which this node lies. In tetrahedral elements, barycentric interpolation is used to discover if the interested node is inside or outside the elements.

In short, barycentric interpolation is a form of tetrahedral interpolation, and barycentric coordinates are the numbers corresponding to the weights placed at the vertices of a tetrahedron. These numbers can be used to determine the location of the center of mass of the tetrahedron corresponding to the weights put on its vertices [10].

Let V_i $(i = 1,2,3,4)$ be the vertices of tetrahedron T . Any point P in three-dimensional space can be expressed as

$$P = \theta_1 V_1 + \theta_2 V_2 + \theta_3 V_3 + \theta_4 V_4 \ , \tag{1}$$

where θ_i's are the barycentric coordinates for point P , and

$$\theta_1 + \theta_2 + \theta_3 + \theta_4 = 1 \ . \tag{2}$$

And point P is inside the tetrahedron if

$$\theta_i > 0 \qquad i = 1,2,3,4 \ . \tag{3}$$

In our problem, point P is a mesh node of Mesh 3, and tetrahedron T is a tetrahedral element of Mesh 2. Thus, V_i and P are known variables in Eqn. (1), and the barycentric coordinates θ_i's are the numbers to be determined. Since the Eqn. (1) can be decomposed into three sub-equations for x, y, and z coordinates, along with Eqn. (2), we therefore have four equations to solve for four barycentric coordinates. Nevertheless, as we search for the element in Mesh 2 that each Mesh 3's node lies inside, we keep the calculated values of barycentric coordinates associated with that node and the element we found as well.

Recall that the initial undeformed mesh (Mesh 1) is deformed into Mesh 2, and both meshes have the same topology. In addition, we now know in which element in Mesh 2 that each Mesh 3's node lies. Therefore, we can map each of these Mesh 3's nodes onto Mesh 1 using Eqn. (1), where θ_i's and V_i are now the known variables, and P is the location of the node to be determined on the undeformed boundary. By mapping all the Mesh 3's nodes onto Mesh 1, the result is the pre-deformed mesh. Fig. 4 depicts the node mapping process in two dimensions.

2.4 Full Analysis

A full analysis is performed on the new pre-deformed mesh obtained from the previous step. Since the pre-deformed mesh is generated using the deformed boundary of the intermediate stage in the pre-analysis, the shape quality of the resulting mesh tends to improve until the maximum point is reached around the stage at which the boundary was taken; then the shape quality starts to degrade. Thus, in cases where the die geometry is complicated, performing the inverse pre-deformation just once might not be enough. However, the inverse pre-deformation method is an iterative method. Therefore, we can use the pre-deforming result as the starting mesh and iteratively perform the pre-deformation until the desired results are obtained. The next section illustrates the inverse pre-deformation method on a test problem, and discusses the results.
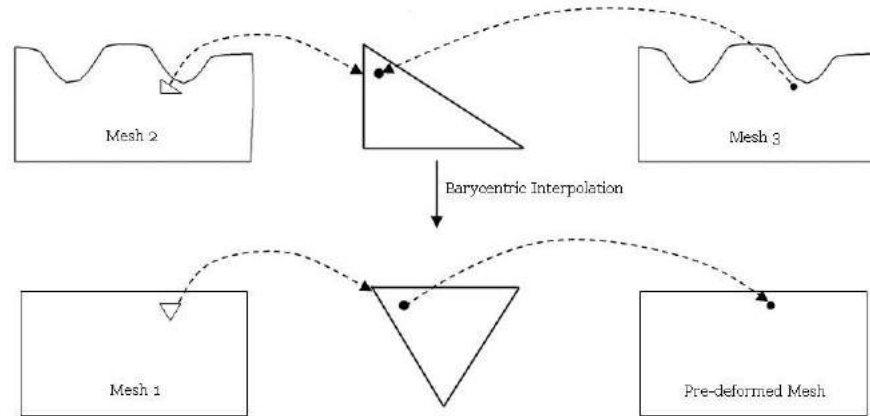
Fig. 4. Node mapping process.

3. COMPUTATIONAL EXPERIMENTS AND DISCUSSION

3.1 Test Problem

Following is the model of the test problem considered in this paper [18]:

The model consists of a sinusoidal rigid die and a 20mm by 10mm by 20mm deformable blank. The bottom of the blank is constrained in the y-direction, and symmetry boundary conditions are applied at the x=0 and z=10 planes. The die has a sinusoidal shape with amplitude and period of 5 and 10 mm, respectively. The material of the blank is steel and modeled as a von Mises elastic-plastic material with a Young's modulus of 200 GPa, an initial yield stress of 100 MPa, and a constant hardening slope of 300 MPa. The Poisson's ratio is 0.3 and the density is 7800 kg/m^3. The die is moved downward vertically at a velocity of 2000 mm/sec and is constrained in all other degrees of freedom. Fig. 5 shows the model geometry of the test problem.
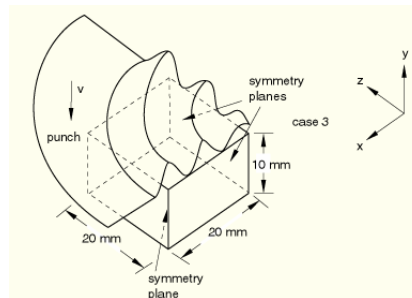
Fig. 5. Model geometries of the test problem.

3.2 Pre-deformed Mesh

We have run three iterations of the inverse pre-deformation on this test problem. The 2nd iteration uses the result in step 9 of the 1st iteration as the starting mesh, and the 3rd iteration uses the result in step 11 of the 2nd iteration as the starting mesh. The first frames of Fig. 6 (b) and (c) show the resultant pre-deformed mesh for the 1st and 3rd iterations respectively. It is shown that the pre-deformed meshes can capture the feature areas of large deformation and pre-deform the elements, as well as refine the element sizes around those locations successfully. Furthermore, these feature areas can be captured more accurately in the later pre-deforming iterations.

(a) Original Mesh   (b) Pre-deformed Mesh (1st iteration)   (c) Pre-deformed Mesh (3rd iteration)
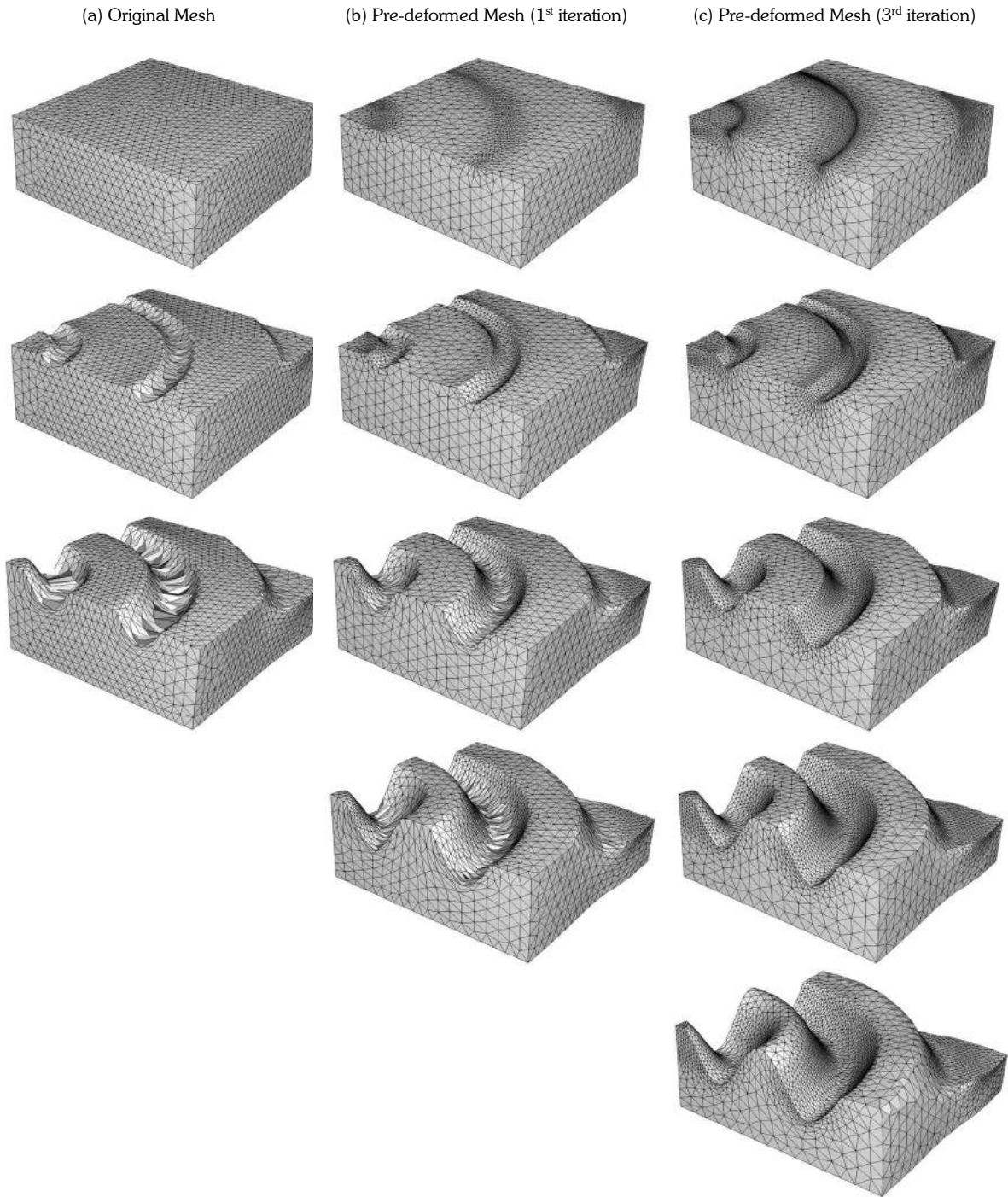
Fig. 6. Finite element analysis of the original mesh (a), 1st iteration pre-deformed mesh (b), and 3rd iteration pre-deformed mesh (c).

3.3 Analysis Results

In this section, the results from the analyses of the pre-deformed meshes are shown and compared with the results from the analysis of the original mesh. Fig. 6 (a), (b) and (c) show the finite element analysis results of the original mesh, the 1st iteration pre-deformed mesh and the 3rd iteration pre-deformed mesh, respectively.

It is demonstrated in Fig. 6 that the analysis of the original mesh begins to produce ill-shaped elements at a very early stage, while the pre-deformed meshes can extend the life of the analysis to the later stages. This is because the thin and fine elements in the pre-deformed meshes, which were intentionally generated at locations expected to encounter high-curvature corners during analysis, gradually unfold as the analysis continues. Consequently, the shapes of the elements tend to improve progressively during the analysis, until at some point in the later analysis steps, element shape quality would begin to degrade.

To compare shape quality of the meshes during analysis of the original mesh, and pre-deformed meshes, the radius ratios are computed. The radius ratio ρ is defined as the ratio of the inradius ρ_{in} and circumradius ρ_{out} of a tetrahedron. The values of ρ_{in} and ρ_{out} can be calculated as

$$\rho_{in} = 3v / \sum_{i=0}^{3} s_i , \tag{4}$$

$$\rho_{out} = \frac{\sqrt{(a+b+c)(a+b-c)(a+c-b)(b+c-a)}}{24v} . \tag{5}$$

Then,

$$\rho = 3\frac{\rho_{in}}{\rho_{out}} = \frac{216v^2}{\sqrt{(a+b+c)(a+b-c)(a+c-b)(b+c-a)} \sum_{i=0}^{3} s_i} , \tag{6}$$

where a, b and c are the products of the lengths of opposite edges of a tetrahedron. [20]

The optimal value of radius ratio is 1, and the high value of radius ratio indicates ill-shaped tetrahedron. The following Tab. 1 shows the percentage of the total elements that have radius ratio greater than 50 at various analysis steps in the test problem.

Step	Original mesh (%)	1st iteration Pre-deformed mesh (%)	2nd iteration Pre-deformed mesh (%)	3rd iteration Pre-deformed mesh (%)
3	0.08	0.07	0.42	0.47
6	0.31	0.14	0.30	0.19
9	0.56	0.40	0.33	0.13
12	0.90	0.79	0.54	0.15
15	1.32	1.30	0.93	0.28
18	1.90	1.90	1.51	0.55

Tab. 1. Percentage of the total elements that have radius ratio greater than 50.

According to Tab. 1, the increasing percentage of original mesh elements implies that the overall shape quality of the original mesh degrades as the analysis continues. The result of the 1st iteration pre-deformed mesh is obviously improved as fewer number of elements have large radius ratio. In the 2nd and 3rd iterations, the pre-deformed meshes start with more elements having large radius ratio, because many elements are deformed in advance to reduce the severe element distortion expected during analysis. Nevertheless, after only a few analysis steps, the shape quality of the pre-deformed meshes improves rapidly, and the pre-deformed mesh results become better than the original mesh results. Fig. 7 illustrates the elements with radius ratio greater than 50 at step 18 for the original and pre-deformed meshes.

(a) Original Mesh   (b) Pre-deformed Mesh (1st iteration)   (c) Pre-deformed Mesh (2nd iteration)   (d) Pre-deformed Mesh (3rd iteration)
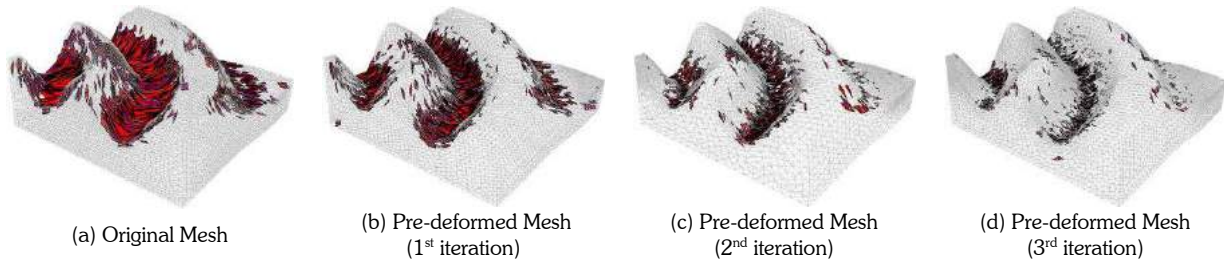
Fig. 7. Elements that have radius ratio greater than 50 at step 18.

Fig. 8 (a) and (b) show the quality histogram of the meshes at analysis step 12 and 18, respectively. It is illustrated in the figures that the pre-deformed meshes increase the number of elements with small radius ratio, and reduce the number of elements with large radius ratio. Therefore, the pre-deformed mesh can help to improve the overall shape quality of the mesh, especially in the later stage of the analysis.

(a) Quality histogram at step 12   (b) Quality histogram at step 18
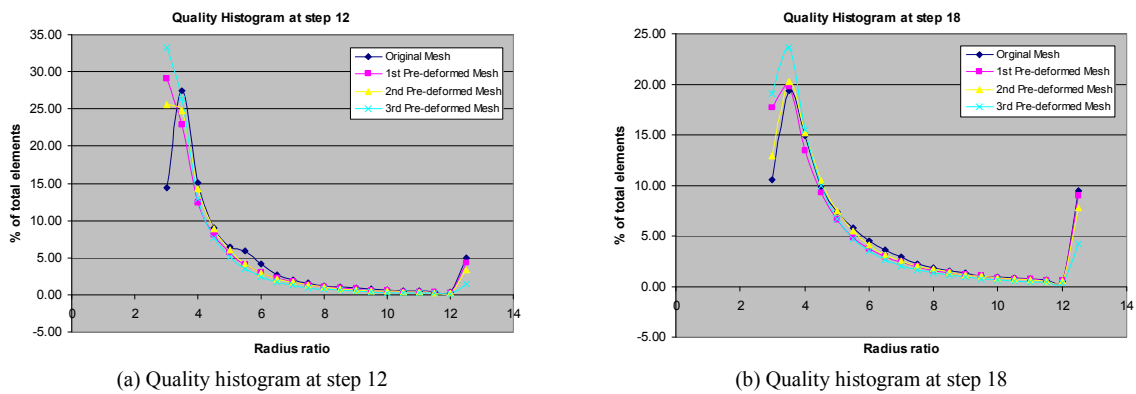
Fig. 8. Quality histogram at analysis step 12 and step 18.

4. CONCLUSION
Summary of the proposed inverse pre-deformation method
- This paper proposes the inverse pre-deformation method, which inversely deforms and refines elements at locations where large deformation is expected in advance.
- The inverse pre-deformation method is an iterative method. In problems with complicated die geometry, the inverse pre-deformation method can be run iteratively to obtain the desired analysis result.

Advantages verified by the computational experiments
- Pre-deformed mesh can help improve the overall shape quality of the mesh during analysis.
- Pre-deformed mesh can extend the analysis life to the further steps than the original mesh, because the shape quality of the meshes at the later stage is improved.
- Because pre-deformed mesh can extend the life of the analysis longer before the mesh become unacceptable, it can help reduce the number of adaptive remeshing required during the analysis.
- Commonly, the users who run this type of analysis have to use their own common sense to determine how the input mesh should be generated in order to keep the analysis run to the desired stage. This pre-deformation method can be a tool to aid them on that purpose.

5. ACKNOWLEDGEMENT

6. REFERENCES

[1]   Jie Wan, Suleyman Kocak and Mark S. Shephard, "Automated Adaptive Forming Simulations", Proceedings, *12th International Meshing Roundtable*, Sandia National Laboratories, pp.323-334, 2003.

[2]   Timo Meinders, "Simulation of Sheet Metal Forming Processes", Chapter 5. Adaptive Remeshing, Canada, 1999.

[3]   Amir R. Khoei and Roland W. Lewis, "Adaptive Finite Element Remeshing in a Large Deformation Analysis of Metal Powder Forming", *International Journal for Numerical Methods in Engineering 45*, pp. 801-820, 1999.

[4]   Christiaan Stoker, "Developments of Arbitrary Lagrangian-Eulerian Method in Non-Linear Solid Mechanics, Applications to Forming Processes", *University of Twente*, ISBN 90-36512646, 1999.

[5]   Abaqus 6.3 Explicit User Manual, Chapter 7.6 Adaptive Meshing.

[6]   M'hamed Souli, Lars Olovsson and Ian Do, "Ale and Fluid-Structure Interaction Capabilities in Ls-Dyna", 7th International Ls-Dyna Users Conference, 2002.

[7]   M'hamed Souli and Lars Olovsson, "Ale and Fluid-Structure Interaction Capabilities in Ls-Dyna", 2002.

[8]   M'hamed Souli, "An Eulerian and Fluid-Structure Coupling Algorithm in Ls-Dyna", 1999.

[9]   Jonas Gomes, Lucia Darsa, Bruno Costa and Luiz Velho, "Warping and Morphing of Graphical Objects", Chapter3: Transformation of Graphical Objects.

[10]   Ilkka Vallinkoski, "The design and implementation of a color management application", Chapter 6 Gamut Mapping Algorithm, MS Thesis, Helsinki University of Technology, 1998. http://www.kolumbus.fi/vallinkoski/ilkka/Thesis/index.html

[11]   Zienkiewicz Oc and Zhu Jz, "The Super-convergent Patch Recovery and a Posteriori Error Estimates, Part1: The Recovery Technique", *International Journal for Numerical Methods in Engineering*, 1992.

[12]   Zienkiewicz Oc and Zhu Jz, "The Super-convergent Patch Recovery and a Posteriori Error Estimates, Part2: Error Estimates and Adaptivity", *International Journal for Numerical Methods in Engineering*, 1992.

[13]   Kenji Shimada and David C. Gossard, "Bubble Mesh: Automated Triangular Meshing of Non-Manifold Geometry by Sphere Packing", *Proceedings of The Third ACM Symposium on Solid Modeling and Applications*, pp. 409-419, 1995.

[14]   Kenji Shimada, Atsushi Yamada, and Takayuki Itoh, "Anisotropic Triangular Meshing of Parametric Surfaces via Close Packing of Ellipsoidal Bubbles", *6th International Meshing Roundtable*, Sandia National Laboratories, pp. 375-390, 1997.

[15]   Soji Yamakawa and Kenji Shimada, "High Quality Anisotropic Tetrahedral Mesh Generation via Ellipsoidal Bubble Packing", Proceedings, *9th International Meshing Roundtable*, Sandia National Laboratories, pp. 263-273, 2000.

[16]   Kenji Shimada, Jia-Huei Liao and Takayuki Itoh, "Quadrilateral Meshing with Directionality Control through the Packing of Square Cells", Proceedings, *7th International Meshing Roundtable*, Sandia National Lab, pp. 61-76, 1998.

[17]   Naveen Viswanath, "Adaptive Anisotropic Quadrilateral Mesh Generation Applied to Surface Approximation", MS Thesis, Carnegie Mellon University, 2000.

[18]   Abaqus Example Problems Manual Version 6.3, Section 1.3.9 Forging with Sinusoidal Die.

[19]   Arbtip Dheeravongkit, Kenji Shimada, "Inverse Pre-Deformation of Finite Element Mesh for Large Deformation Analysis", Proceedings, *13th International Meshing Roundtable*, Sandia National Laboratories, pp. 81-94, 2004.

[20]   J.Dompierre, P.L., F. Guibault, R. Camerero, "Proposal of benchmarks for 3D unstructured tetrahedral mesh optimization", Proceedings, *7th International Meshing Roundtable*, Sandia National Laboratories, pp. 495-478, 1998.